Journal of Materials Chemistry
www.rsc.org/materials

Controlled synthesis of crystalline tellurium nanorods, nanowires, nanobelts and related structures by a self-seeding solution process

Ujjal K. Gautam[a,b] **and C. N. R. Rao***[a,b]

[a]*Solid State and Structural Chemistry Unit, Indian Institute of Science, Bangalore 560012, India. E-mail: cnrrao@jncasr.ac.in*
[b]*Chemistry and Physics of Materials Unit and CSIR Centre of Excellence in Chemistry, Jawaharlal Nehru Centre for Advanced Scientific Research, Jakkur P. O., Bangalore 540064, India*

Received 5th April 2004, Accepted 12th May 2004
First published as an Advance Article on the web 14th June 2004

Single crystalline nanorods and nanowires of *t*-Te have been prepared by a simple solution route. The procedure involves the disproportionation of NaHTe, prepared by the reduction of Te with $NaBH_4$. By carefully controlling the reaction conditions, the diameter of the nanorods could be varied in the 20–300 nm range. Nanowires of 10 nm diameter were obtained in the presence of sodium dodecylbenzenesulfonate. Te nanobelts and nano junctions were obtained by employing hydrothermal and solvothermal conditions. The nanorods have been characterized by a variety of microscopic and spectroscopic techniques. UV-Visible spectra reveal two absorption bands, one around 300 nm which is size-sensitive and the other at 600 nm insensitive to size.

Introduction

There has been a surge of research activity related to the synthesis and characterization of nanorods and nanowires of various inorganic materials such as oxides, sulfides and nitrides as well as elemental materials.[1–3] Among the elemental materials, nanowires of metals such as Au, Ag and Bi as well as non-metals such as Se have been prepared and characterized. One of the elemental materials of interest is tellurium which has several interesting chemical and physical properties including photoconductivity and catalytic activity as well as piezoelectric, thermoelectric and non-linear optical responses.[4,5] Trigonal tellurium (*t*-Te) has an anisotropic crystal structure consisting of helical chains of covalently bonded Te atoms which are bound together through van der Waals interactions in a hexagonal lattice.[5] As a result, *t*-Te would be expected to have a tendency to form 1D structures. Such 1D structures are formed readily from the vapor phase when deposited on a solid substrate.[6] The detailed morphology of the product, however, depends on the temperature and other reaction conditions. Solution phase synthesis has been shown to yield various 1D structures of *t*-Te, depending on the reaction parameters. Thus, Liu *et al.*[7] have prepared nanorods of Te by reducing ammonium sulfotellurate in the presence of sodium sulfite and a suitable surfactant. Nanorods of diameter in the range of 7–30 nm have been obtained by this method. Mayers and Xia[8] have obtained 1D nanostructures of various morphologies by the reduction of orthotelluric acid with hydrazine. This procedure yields nanostructures of varying diameters with lengths of several microns, depending on the solvent and temperature of the reaction. Tellurium nanotubes with diameters in the range of 50–260 nm have been prepared by the polyol process.[9] Disproportionation of Na_2TeO_3 under hydrothermal conditions is shown to yield nanobelts of 30–500 nm width and 8 nm thickness as well as nanotubes of 150–400 nm diameter.[10] Li and coworkers have recently reported preparation of single crystalline Te microtubes by a physical evaporation method.[11] We have been able to prepare nanorods, nanowires and related structures of Te by a very simple strategy involving the disproportionation of sodium hydrogen telluride in aqueous solution at room temperature. By using a surfactant and variety of solvents, 1D nanostructures such as nanobelts and Y-junctions are obtained under hydrothermal or solvothermal conditions. We have previously reported synthesis of various 1D nanostructures of selenium using a similar strategy.[12]

Experimental

Materials

Tellurium (99.99%) and sodium dodecylbenzenesulfonate (99.9%, Aldrich) and $NaBH_4$ (98%, S.D. Fine Chem Ltd.) were used for synthesis without further purification. The reactions were carried out in deionized 18 MΩ water (Easypure R.F., Burnstead).

Synthesis in aqueous medium

In a typical synthesis, 0.0300 g (0.234 mmol) of Te was taken in 20 ml of deionized water in a 250 ml three necked round bottom flask fitted to a nitrogen cylinder. The flask was purged with nitrogen thoroughly. This was heated to 90 °C. 0.0500 g (1.3 mmol) of $NaBH_4$ was added to the flask and the reaction mixture was again purged with nitrogen. The solution turned black immediately accompanied by brisk effervescence. The solution turned pink and after a period of 30 minutes, all the Te dissolved. The solution was diluted, as required, with deionized water heated to the reaction temperature and then the reaction solution was brought to room temperature by natural cooling. Any unreacted Te was filtered off. The solution slowly turns blue. This solution was aged for a predetermined period in order to precipitate out the Te nanophases. The product which settled down at the bottom of the reaction vessel was washed several times with deionized water and air-dried before further characterization. This product generally contained nanorods.

Te nanowires (larger aspect ratios compared to the nanorods) could be obtained when the above procedure was carried

DOI: 10.1039/b405006a

out in the presence of sodium dodecylbenzenesulfonate (NaDBS). In order to achieve this, 0.02 g of NaDBS was added along with the $NaBH_4$ to the reaction mixture described above. The final blue solution was diluted with 40 ml water, cooled to room temperature and kept as such for one week.

Synthesis in a non-aqueous medium

Synthesis of Te nanorods was carried out at 150 °C under refluxing conditions in ethylene glycol or diethylene glycol for two hours. The quantities of the reactants were the same as in the aqueous synthesis. The reaction mixture was cooled to room temperature after refluxing for 2 hours and the resulting solution was kept as such for one week.

Hydrothermal and solvothermal synthesis

Hydrothermal synthesis was carried out in a 40 ml Telfon lined stainless steel autoclave. In a typical reaction, 0.0150 g of Te was mixed with 0.05 g of $NaBH_4$ and 0.02 g of NaDBS in 25 ml of water in an autoclave. This was placed in a hot air oven which was preheated to 150 °C. After 10 hours of heating the autoclave was taken out of the oven and allowed to cool to room temperature in ambient conditions. The product obtained was washed with water several times by centrifugation and subsequent decantation. Reaction was also carried out in presence of 0.10 g of NaDBS and at 200 °C. As discussed later, presence of excess of NaDBS and higher reaction temperature results in aligned nanobelts. Reactions were carried out under identical conditions using ethylene glycol and diethylene glycol as solvents in the absence of NaDBS.

Characterization

Powder X-ray diffraction (XRD) patterns were recorded on a Siemens5005 diffractometer employing the Bragg–Brentano reflection geometry with CuKα radiation (λ = 1.5418 Å). X-Ray photoelectron spectra (XPS) were recorded in an ESCA-3 Mark II spectrometer (GV Scientific Limited, UK) using Al-Kα radiation. Scanning electron microscope (SEM) images were recorded with a JEOL scanning electron microscope. The nanorods were mounted on a brass slab or on clean glass slides, which were further sputter coated with gold to improve conductivity. For the energy dispersive X-ray (EDAX) analysis, uncoated samples were used. The transmission electron microscope (TEM) images were recorded using a JEOL (JEM3010) transmission electron microscope operating with an accelerating voltage of 300 kV. A dispersion of the samples in water was evaporated on a holey carbon grid for this purpose. UV-Vis absorption spectra of the sample-dispersions in water were recorded using a Perkin-Elmer UV-visible spectrometer. The photoluminescence spectra of the samples were recorded using a Perkin-Elmer LS55 spectrophotometer.

Results and discussion

Aqueous synthesis

The reaction of Te (0.030 g) with $NaBH_4$ (0.050 g) in 20 ml of water gave uniform nanowires of 100–300 nm diameter with lengths of ~10 μm. The nanorods precipitated out as soon as the pink solution (see Experimental) was cooled. The lengths of the nanorods were, however, not uniform at this stage and the surfaces were not smooth. On keeping the blue-colored solution at room temperature for 2 days, the supernatant liquid became colorless and nanorods settled down in the reaction vessel. These nanorods were smooth and uniform as shown in the SEM image in Fig. 1a. The peaks in the XRD pattern (Fig. 2) could be indexed on a hexagonal cell (space group $P3121$, JCPDS 36-1452). The X-ray photoelectron spectrum of the nanorods gave two peaks at 573.6 and 583.8 eV

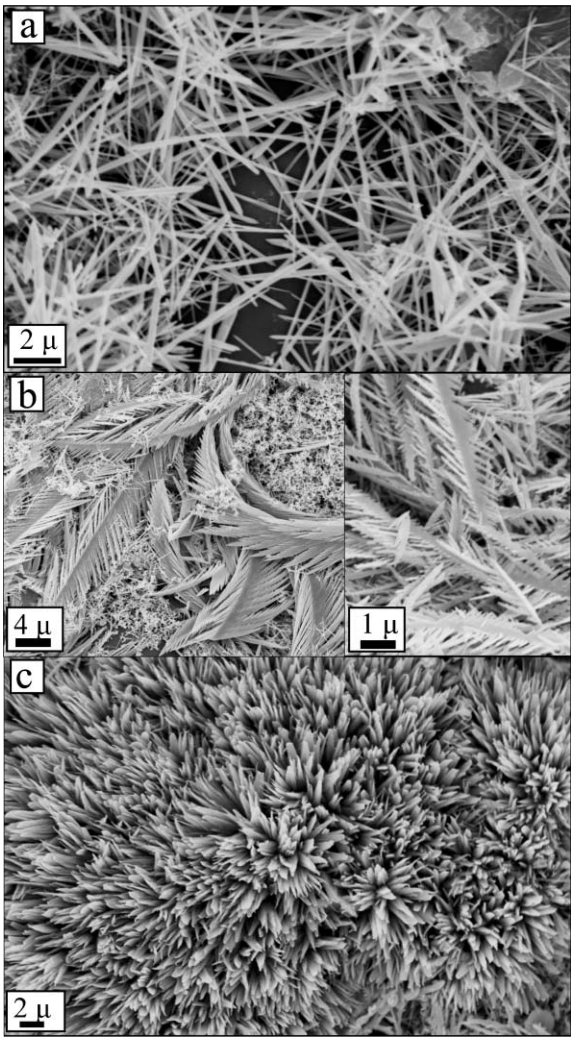

Fig. 1 SEM images of (a) the nanorods obtained from the reaction of 0.03 g of Te with $NaBH_4$ in 20 ml water, (b) feather-like structures obtained with high reactant concentrations (0.3 g of Te powder in 20 ml of water) and of (c) *t*-Te nanoflowers.

corresponding to the Te(0) $3d^{5/2}$ and $3d^{3/2}$ states respectively. XPS studies also revealed the absence of boron and sodium. The EDAX analysis also confirmed that the product is free from recognizable impurities. In Fig. 3a we show a TEM image of the Te nanorods. The electron diffraction (ED) pattern of the rods (see inset in Fig. 3a) confirms the single crystalline nature of the rods. The diffraction spots could be indexed on the basis of the hexagonal structure. Fig. 3b shows a high resolution electron microscope (HREM) image of one of the nanorods. The fringe spacing of 5.8 Å observed in the image corresponds to the separation between the [001] lattice planes of hexagonal Te. The image reveals that the growth of the nanorods is perpendicular to [001] planes.

It would be relevant to examine the reactions involved in aqueous synthesis. Te powder reacts with $NaBH_4$ leading to the formation of NaHTe in solution, just as NaHSe is formed from Se and $NaBH_4$.[13] The NaHTe solution disproportionates producing amorphous Te (*a*-Te) nanoparticles of ~50 nm diameter or less. *a*-Te with high surface energy dissolves away, first giving rise to *t*-Te seeds of 20–300 nm diameter depending upon the reaction conditions. The lateral dimensions of the 1D structures formed in due course depend on the nature of the seeds and can be varied by varying the initial reaction conditions. The transformation of *a*-Te starts soon after its formation. However, the kinetics of the *a*-Te–*t*-Te transformation depends on the concentration of Te in solution. When 20 mg Te was reacted in 20 ml of water, the

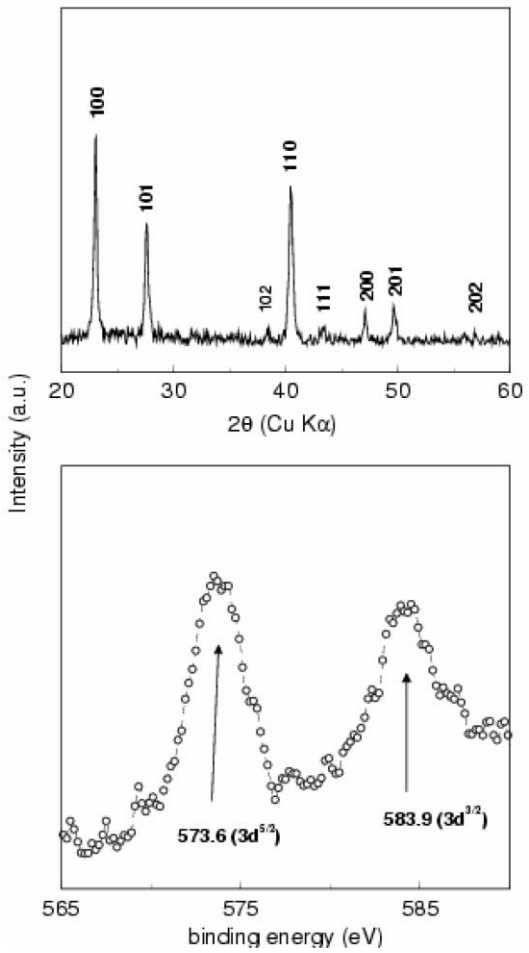

Fig. 2 (a) Powder XRD pattern of *t*-Te nanorods of 300 nm diameter, (b) X-ray photoelectron spectrum of the nanorods.

transformation was complete in ~48 hours, while it took about a week when the same reaction mixture was diluted with 150 ml of water. The rate of transformation slows down at low temperatures. In Fig. 4a, we show the formation of *t*-Te nanorods schematically. A likely reaction scheme is as follows:

$$4NaBH_4 + 2Te + 7H_2O \rightarrow 2NaHTe + Na_2B_4O_7 + 14H_2 \quad (1)$$

$$Na_2B_4O_7 + 2NaHTe + 2Te + 5H_2O \rightarrow 2Na_2Te_2 + 4H_3BO_3 \quad (2)$$

$$Na_2Te_2 + 2H_2O \rightarrow 2a\text{-Te} + 2NaOH + H_2 \quad (3)$$

$$a\text{-Te} \rightarrow t\text{-Te} \quad (4)$$

The dimensions of the Te nanorods obtained in aqueous synthesis depend primarily on the initial concentrations of the reactants. Thus, when the reaction was carried out with 0.300 g of Te powder and 0.500 g of $NaBH_4$ in 20 ml of water, interesting morphologies were obtained. In Fig. 1b, we show a SEM image of the feather-like structures obtained in such a preparation. The abundance of amorphous tellurium in the solution mixture results in rapid precipitation leading to bigger rod-like structures. Such precipitation may give rise to defects which act as nuclei for further growth leading to feather-like structures. Interestingly we have observed that around 10% of the product floats on the surface of the solution soon after the reaction mixture is kept for cooling. The floating material composes of *t*-Te nanoflowers as shown in SEM image in Fig. 1c. The nano-flowers resemble the f-whiskers or filamentary crystallites with tapered tips and broad bases, similar to the structures reported by Futura *et al.*[6] in the vapor phase

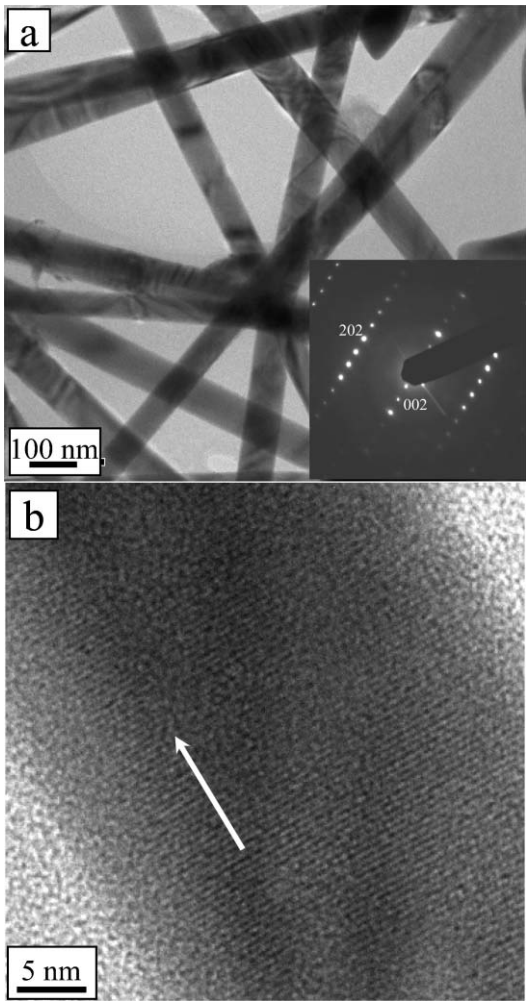

Fig. 3 (a) TEM image of the *t*-Te nanorods obtained by reacting 0.03 g of Te with 0.05 g of $NaBH_4$ in 20 ml water and without further dilution. Inset shows the electron diffraction pattern of a nanorod showing its single crystalline nature. (b) HREM image of a nanorod showing the [001] lattice planes of hexagonal Te.

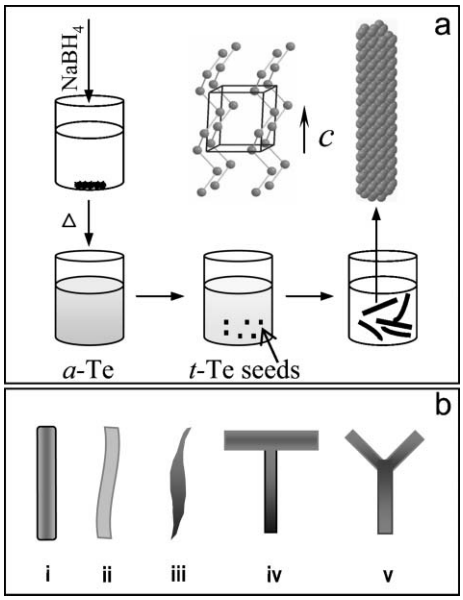

Fig. 4 (a) Schematic of the process of formation of *t*-Te nanorods. Addition of $NaBH_4$ to a container with Te powder in water upon heating leads to an aqueous solution of NaHTe. (b) By appropriate control of the reaction conditions, different morphologies of the 1D nanostructures of Te are achieved: (i) rods or wires, (ii) belts, (iii) tapered rods or whiskers, (iv) T-junctions and (v) Y-junctions.

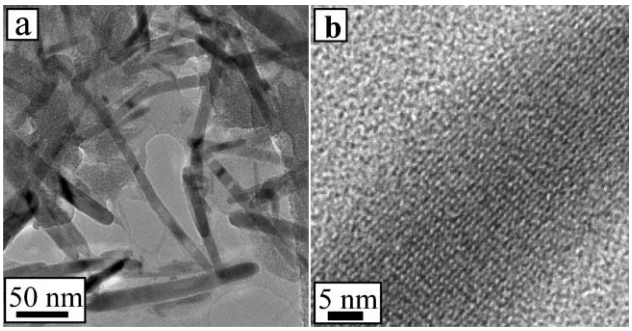

Fig. 5 (a) TEM image of nanorods of 20 nm diameter obtained as a result of subsequent dilution of the reaction of 0.03 g of Te in 20 ml water. (b) HREM image of a nanorod revealing its single crystalline nature.

synthesis. In addition to nanorods, other types of nanostructures such as tapered rods, nanobelts, whiskers and Y-junctions (Fig. 4b) are obtained from aqueous synthesis, depending on the reaction conditions.

Nanorods of smaller dimensions were obtained when low initial concentrations of the reactants were employed. For example, when a reaction mixture of 0.030 g of Te powder and 0.050 g of $NaBH_4$ was diluted with 150 ml of hot deionized water, just after the dissolution of the Te powder, we obtained uniform nanorods of 20 nm diameter and 400 nm length. The solution became blue and remained stable for long periods. A TEM image of the nanorods obtained from a solution kept for a month is shown in the Fig. 5a. The rods are highly crystalline as revealed by the HREM image shown in Fig. 5b.

Nanowires with high aspect ratios were obtained when (see Experimental) sodium dodecylbenzenesulfonate (NaDBS) was added to the aqueous reaction mixture. A TEM image of the nanorods obtained by this method is shown in Fig. 6a. The wires were fairly monodisperse with a mean diameter of 10 nm while their lengths extended to several microns. Some of the nanowires were bent, while others were straight (Fig. 6b). HREM images (see inset of Fig. 6b) reveal the nanowires to be single crystalline growing along the <001> direction of the hexagonal Te structure. The exact role of NaDBS in the formation of the nanowires is not clear, although surfactant-assisted growth of such inorganic nanowires is well documented.[3,14–15]

The reaction of Te powder with $NaBH_4$ was carried out in ethylene glycol as well as in diethylene glycol. While in ethylene glycol, the reaction was slow and yielded nanorods of 20 nm diameter and 300 nm length, the reaction in ethylene glycol was highly incomplete leaving behind unreacted Te.

Optical properties of nanorods

Optical absorption spectra of Te have been studied by a few coworkers. Isomaski *et al.*[16] have reported an absorption band in the range of 0–3 eV due to the transition from the valence band (*p*-nonbonding triplet) to the conduction band (*p*-antibonding triplet), and a band in the 3–6 eV range due to the valence band (*p*-bonding triplet) to the conduction band (*p*-antibonding triplet). Swan *et al.*[17] have studied the absorption spectra for thin films. These workers report characteristic absorption peaks at 2.21 eV and 4.60 eV, with the first band assigned to a forbidden direct transition and the other to an allowed direct transition. We have recorded the electronic absorption spectra of the Te nanorods and nanowires. The spectra show a characteristic absorption band in the 250–350 nm (4.9–3.5 eV) range which is sensitive to the diameter of the nanorods. Bulk samples of Te shows a broad absorption maximum around 300 nm. In Fig. 7, we show typical absorption spectra of the nanorods. The spectrum of the nanorods of 300 nm diameter is similar to that of the bulk.

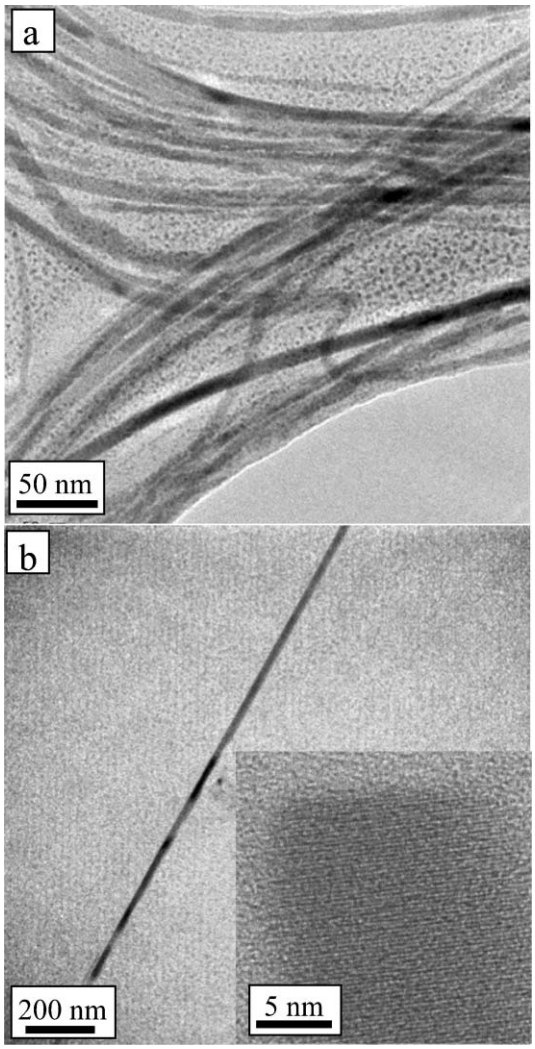

Fig. 6 (a) TEM image of nanowires obtained in presence of the surfactant NaDBS when the reaction was carried out with 0.03 g of Te powder. (b) TEM image of a straight nanowire. Inset shows the tip of this nanowire with well-resolved [100] planes.

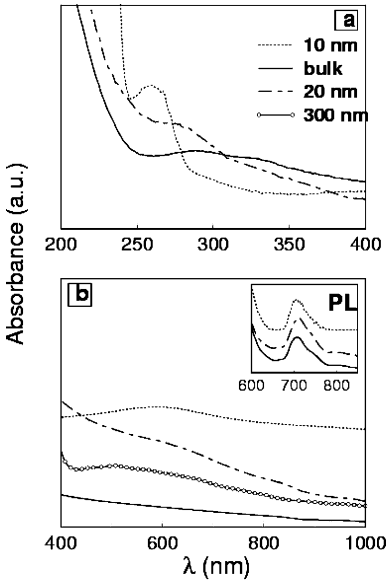

Fig. 7 (a) The size dependent UV-visible spectra of Te nanorods in the 200–400 nm range. (b) Spectra of the nanorods in the range 400–1000 nm. The broad band at 600 nm (not observed in the spectrum of the bulk) is size independent and occurs in the spectra of nanorod samples. Inset shows the PL spectra of the nanorods.

The 20 nm nanorods have an absorption maximum at 270 nm. Nanowires of 10 nm diameter show a further shift in the absorption maximum to around 260 nm. We also observe a broad band around 600 nm (2 eV), whose position is not sensitive to the size of the nanorods (Fig. 7b). The nature and origin of these bands are, however, not clear at present.

Photoluminescence spectra of the Te nanorods were recorded with excitation wavelengths of 300 and 600 nm. We observed emission bands at 700 nm at both the excitation wavelengths (see inset in Fig. 7b), but the position of the band was insensitive to size.

Hydrothermal and solvothermal synthesis

Unlike the solution phase synthesis, where uniform nanorods were obtained, hydrothermal synthesis (see Experimental) yielded crystalline Te nanobelts as shown in the TEM image in Fig. 8. The product consisted mostly of nanobelts (70%) and a few nanorods. The nanobelts are uniform in dimensions with widths of 50–100 nm and lengths of 1–10 microns. The thickness of the belts is estimated to be in the 5–10 nm range. An interesting feature of the nanobelts is their tendency to form branches and junctions as shown in Fig. 8a, b and c. Around 15% of the nanobelts exhibit such junctions. Mo *et al.*[10] have reported nanobelts of Te prepared hydrothermally at 180 °C. These workers observed that when the temperature of the reaction was increased to 230 °C, nanorods are formed. We recall that the reactions in aqueous media yielded nanorods even at 90 °C. Nanobelts, on the other hand, were obtained at 150 °C under hydrothermal conditions.

An interesting feature of the hydrothermal synthesis is the yield of aligned nanobelts at a higher temperature in the presence of excess surfactant. In Fig. 9a, we show the SEM image of the nanobelts obtained by this means. Each nanobelt in the image is a collection of aligned nanobelts of much smaller widths. The TEM images reveal that the nanobelts have an average width of 10 nm with lengths of several microns (Fig. 9b and c). These nanobelts form stable dispersions in water for months. Control of morphology and self-assembly of nanostructures using functionalized organic additives is well documented.[18] In the case of aligned nanobelts of Te, the oxygens of the sulfate group in NaDBS moieties interact with

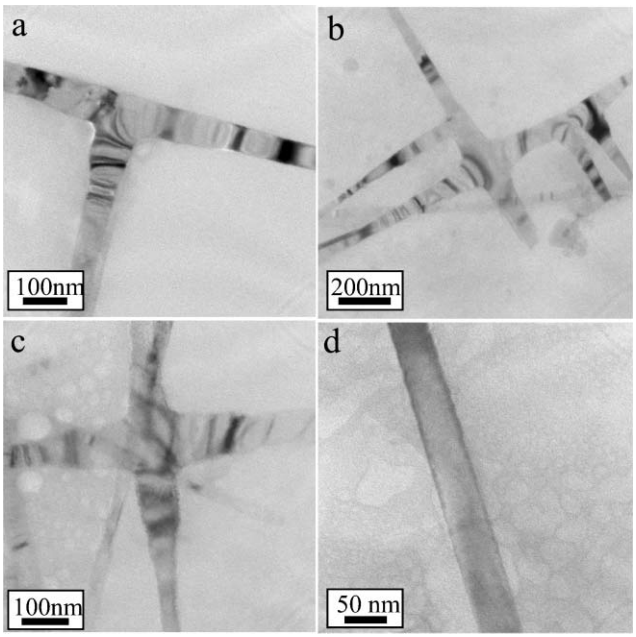

Fig. 8 Nanobelts of *t*-Te containing T-junctions and similar structures obtained by hydrothermal synthesis. (a), (b) and (c) show TEM images of such structures. (d) TEM image of a single nanobelt. Inset shows tip of a nanobelt.

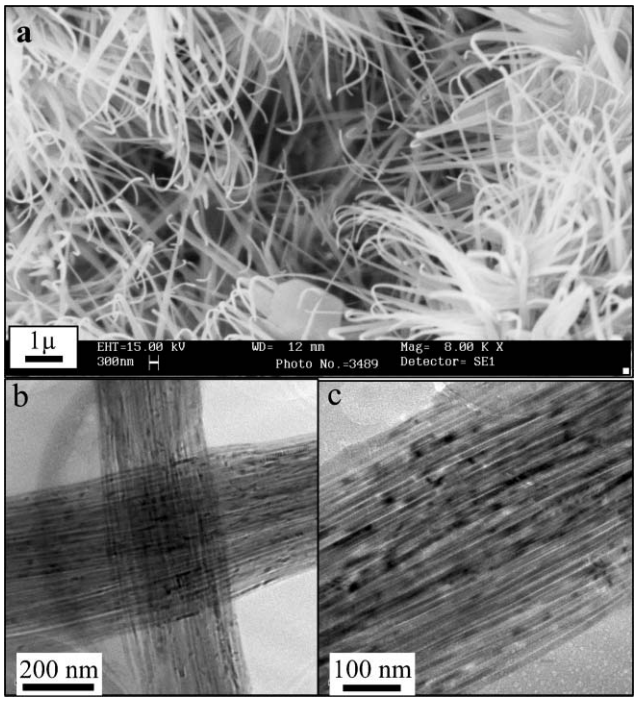

Fig. 9 (a) SEM image and (b) and (c) TEM images of aligned nanobelts of Te.

Te atoms along *ac* and *bc* planes of the unit cell. The lateral dimensions of the nanobelts therefore decreases considerably. The hydrophobic chains of the surfactant (in water) assist the formation of the aligned nanoassemblies of the belts.

Solvothermal synthesis (see Experimental) in diethyleneglycol also gave nanobelts. A TEM investigation of the product obtained from the solvothermal reaction in diethylene glycol shows the formation of nanobelts along with junctions (see Fig. 10a–c). The nanobelts are not as uniform as the ones obtained under hydrothermal synthesis. When the solvothermal reaction was carried out in ethylene glycol under similar conditions, the reaction was incomplete, but yielded nanostructures including junctions (see Fig. 10d). The high pressure generated in hydro/solvothermal reactions[19] may be a factor in determining the morphology of the Te-nanostructures.

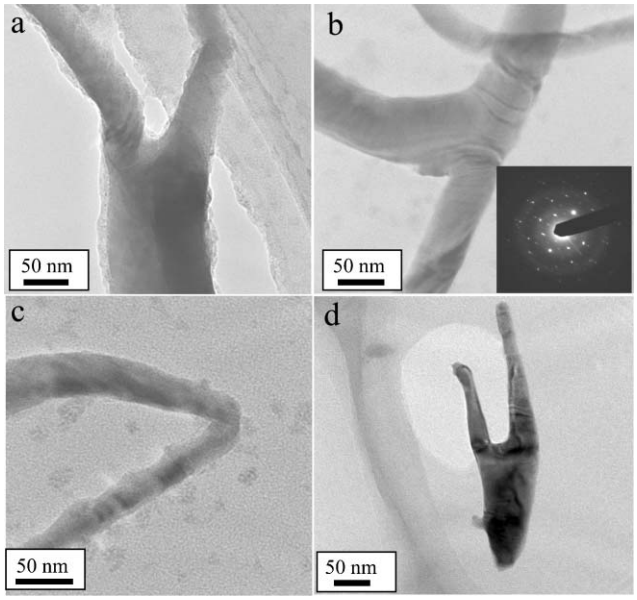

Fig. 10 TEM images (a), (b) of Y-junctions obtained solvothermally by using diethylene glycol as solvent. Inset shows the ED pattern of a junction, (c) of a bent nanobelt and (d) of a junction obtained using ethylene glycol as solvent.

Conclusions

Single crystalline, one-dimensional nanostructures of *t*-Te have been prepared by a simple procedure involving the reaction of Te powder with $NaBH_4$. In aqueous media at 90 °C the method yields uniform nanorods. The same reaction under hydrothermal conditions yields nanobelts and junctions of various shapes. The simplicity of the reaction involving inexpensive and non-hazardous chemicals and the total conversion of the reactants to nanostructures renders the present procedure attractive. Presence of surfactant in the reaction greatly affects the morphology of the nanostructures, enabling the synthesis of nanowires with high aspect ratios and aligned nanobelts. The present procedure can be usefully employed to synthesize nanostructures of SeTe alloys.

Acknowledgements

The authors thank DRDO (India) for research support. U. K. G. thanks Council of Scientific and Industrial Research, India for granting a senior research fellowship.

References

1 Y. Xia, P. Yang, Y. Sun, Y. Wu, B. Mayers, B. Gates, Y. Yin, F. Kim and H. Yan, *Adv. Mater.*, 2003, **15**, 353.
2 Z. L. Wang, *Adv. Mater.*, 2000, **12**, 1295.
3 C. N. R. Rao, F. L. Deepak, G. Gundiah and A. Govindaraj, *Prog. Solid State Chem.*, 2003, **31**, 5.
4 E. Gerlach and P. Grosse, *The physics of selenium and tellurium*, Springer-Verlag, Berlin Heidelberg. 1979.
5 E. D. Cooper, *Tellurium*, Van Nostrand Reinhold Co., New York, 1974.
6 N. Futura, Y. Ohashi, H. Itinose and Y. Igarashi, *Jpn. J. Appl. Phys.*, 1975, **11**, 929.
7 Z. Liu, Z. Hu, Q. Xie, B. Yang, J. Wu and Y. Qian, *J. Mater. Chem.*, 2003, **13**, 159.
8 B. Mayers and Y. Xia, *J. Mater. Chem.*, 2002, **12**, 1875.
9 B. Mayers and Y. Xia, *Adv. Mater.*, 2002, **14**, 279.
10 M. Mo, J. Zeng, X. Liu, W. Yu, S. Zhang and Y. Qian, *Adv. Mater*, 2002, **14**, 1658.
11 X.-L. Li, G.-H. Cao, C.-M. Feng and Y.-D. Li, *J. Mater. Chem.*, 2004, **14**, 244.
12 U. K. Gautam, M. Nath and C. N. R. Rao, *J. Mater. Chem.*, 2003, **13**, 2845.
13 D. L. Klayman and T. S. Griffin, *J. Am. Chem. Soc.*, 1973, **95**, 197.
14 L. M. Qi, J. M. Ma, H. M. Cheng and J. G. Zhao, *J. Phys. Chem. B*, 2001, **105**, 4065.
15 N. R. Jana, L. Gearheart and C. J. Murphy, *Adv. Mater.*, 2001, **13**, 1389.
16 H. M. Isomaski and J. von Boehm, *Phys. Scr.*, 1982, **25**, 801.
17 R. Swan, A. K. Ray and C. A. Hogarth, *Phys. Status Solidi A*, 1991, **127**, 555.
18 S.-H. Yu, H. Colfen and M. Antonietti, *Chem. Eur. J.*, 2002, **8**, 2937.
19 M. Rajamathi and R. Seshadri, *Curr. Opin. Solid State Sci.*, 2002, **6**, 337.